

An Aneroid Pressure Sensor for Constant-Level Balloons

NADAV LEVANON,¹ JURIS AFANASJEVS, ROBERT A. OEHLKERS AND VERNER E. SUOMI

Space Science and Engineering Center, University of Wisconsin, Madison 53706

(Manuscript received 21 August 1974, in revised form 3 February 1975)

ABSTRACT

The pressure sensor for the Tropical Wind Energy conversion and Reference Level Experiment (TWERLE) is described. Key design features of the sensor are: capacitive coupling, reference at midrange, up-down counting, passive oven, storage at flight pressure and prelaunch calibration. Sensor specifications are given which are based on the production results of 440 units. Drift, as estimated from simulated life tests, is 1 mb per 6 months. The overall weight of the sensor, including thermal package, is 180 g.

1. Introduction

The pressure sensor described here was designed and built for the Tropical Wind Energy conversion and Reference Level Experiment (TWERLE). In this experiment, scheduled for launch in 1975, 400 super-pressure balloons will be launched in the Southern Hemisphere to a flight level near 150 mb.

Cost and weight considerations narrow the choice of the sensing device to the radiosonde type of metal aneroid capsule. To minimize mechanical loading on the sensor a capacitive coupling was selected between the capsule and the electronics. The aneroid capacitor serves as the tuning capacitor of a Clapp oscillator. The rest of the circuitry includes a source follower buffer and a complementary output stage.

To minimize the effects of oscillator drift, the aneroid capacitor is compared to a reference capacitor. The difference between the reference frequency and the aneroid frequency is a measure of pressure. The oscillator effect will be completely nullified if the two capacitors (or two frequencies) are equal. The reference capacitor is a system of three capacitors, one of them variable. The variable capacitor is adjusted for zero frequency difference at the expected flight pressure of 150 mb.

The frequency difference is measured by an external up-down counter with an equal gate time for the reference frequency, which is counted down, and for the aneroid frequency, which is counted up.

Extensive comparison tests were conducted between the Vaisala and VIZ radiosonde capsules. Both capsules yielded very similar results with respect to short- and long-term stability, and temperature coefficient. The Vaisala 150 mb capsule was chosen because it is

supplied with its coupling capacitor already mounted. Typical values for the sensor are: reference frequency of 1 MHz, sensitivity of 400 Hz mb⁻¹ and temperature dependence of +0.06 mb °C⁻¹. A thermistor is attached to the aneroid mount. It is connected to a separate temperature measuring circuit to yield the pressure sensor temperature within 1°C.

To allow maximum pre-flight aging at the expected pressure level, the aneroid capsule is mounted inside an evacuated bubble which has a modified relief valve. From the assembly stage, throughout the temperature cycling, calibration, storage, prelaunch calibration, and balloon ascent, the aneroid is never again exposed to surface pressure. (However, accidental exposure, for short periods, is not harmful.) The relief valve opens at a pressure differential of 60 mb. Hence, it will only open during the balloon ascent just prior to arrival at the ceiling altitude.

In addition to the temperature compensation and temperature monitoring, the entire pressure sensor is enclosed in a passive temperature enclosure. A spherical enclosure was chosen after tests of various types in actual balloon flights, to find the lowest, flattest, and most stable daytime temperature curve.

Special care is devoted to the calibration. The calibration is performed after four days of temperature cycling and four days of simulated flight conditions. In addition, a correction is made after a pre-launch calibration.

2. General description

The pressure sensor is constructed from three parts: The aneroid capsule (Fig. 1) enclosed in a Lexan² bubble, the electronics board (Fig. 2), and the spherical styrofoam package (Fig. 3).

¹ Present affiliation: Department of Environmental Sciences, Tel-Aviv University, Ramat Aviv, Israel.

² Trademark of General Electric Co.

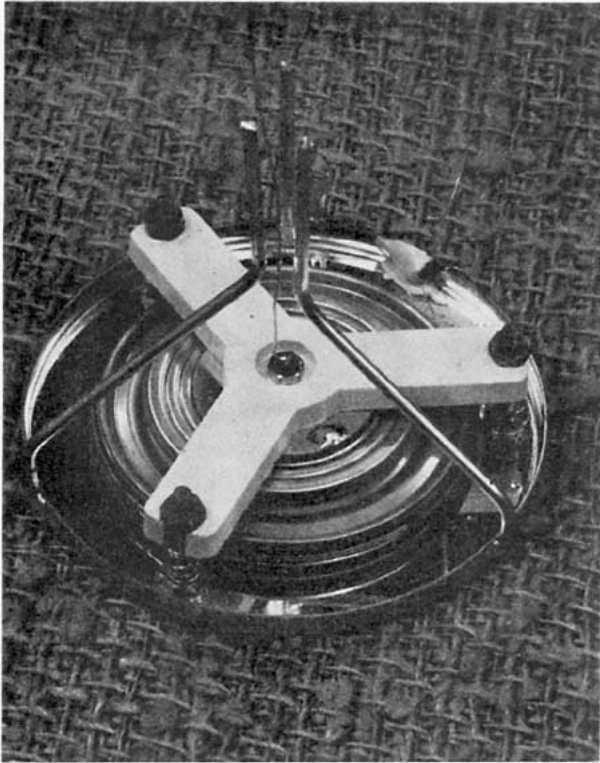


FIG. 1. The Vaisala aneroid capsule.

The aneroid capsule is mounted as supplied. The thermistor is glued to the base of the mount, and three wire mounting struts are used to support the capsule inside the bubble. The two halves of the bubble are vacuum formed on molds, using a 0.06-inch Lexan sheet. A hole at the bottom of the spherical styrofoam package provides access to the relief valve. The valve is also the bubble outlet for vacuum pumping.

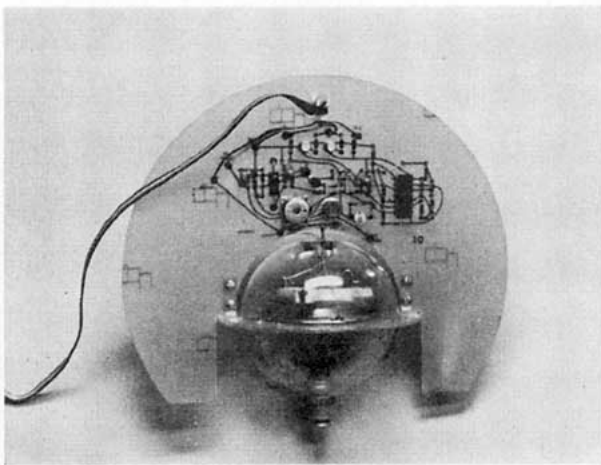


FIG. 2. The pressure sensor electronics, aneroid, bubble, and relief valve.

When completely assembled the aneroid capsule is horizontally positioned. This configuration yielded a dependence of the pressure reading on the tilt angle of only $0.002 \text{ mb } ^\circ\text{C}^{-1}$. A vertical positioning was more sensitive to tilt by a factor of 4.

A complete electrical schematic diagram of the pressure sensor is given in Fig. 4. The reference capacitor or the aneroid capacitor, depending on the switch position, comprises the tuning capacitor of a Clapp oscillator whose output is buffered by a source follower. Both stages are constantly on. Hard limiting is provided by three stages of a COS/MOS buffer integrated circuit which are connected serially. The output stage is a complementary emitter follower. The hard limiter and the output stage are turned on 1.28 s before a pressure reading is taken. After this settling down period the output frequency is counted down for a gate period of 1.28 s. During the next (third) 1.28 s the relay is activated, switching the tank circuit from the reference capacitor to the aneroid capacitor. During the fourth period of 1.28 s, the output frequency is counted up in the same counter, leaving in the counter the difference between f_{aneroid} and $f_{\text{reference}}$. The control and counting circuitry are part of the balloon encoder and do not appear in the schematic diagram.

3. Minimizing the effect of temperature variations

a. Nulling

There are three contributing components to the pressure reading error: change in the aneroid capacitor, change in the reference capacitor, and change in the remaining oscillator circuitry. The errors contributed by the first two could be reduced only by selecting better components. However, the role of the oscillator circuitry can be completely nullified if the reference

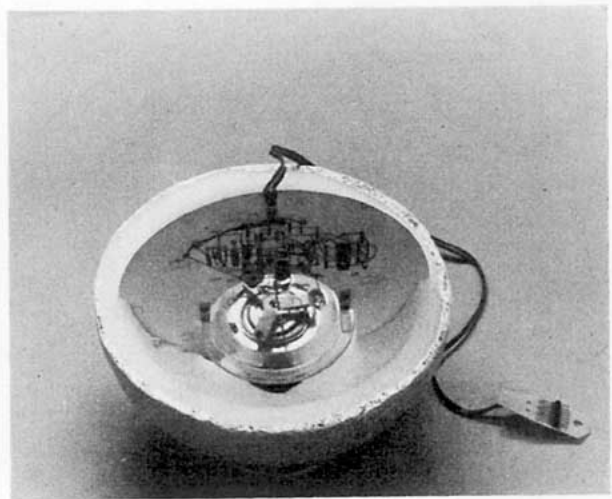


FIG. 3. The TWERLE pressure sensor (upper hemisphere of the package removed).

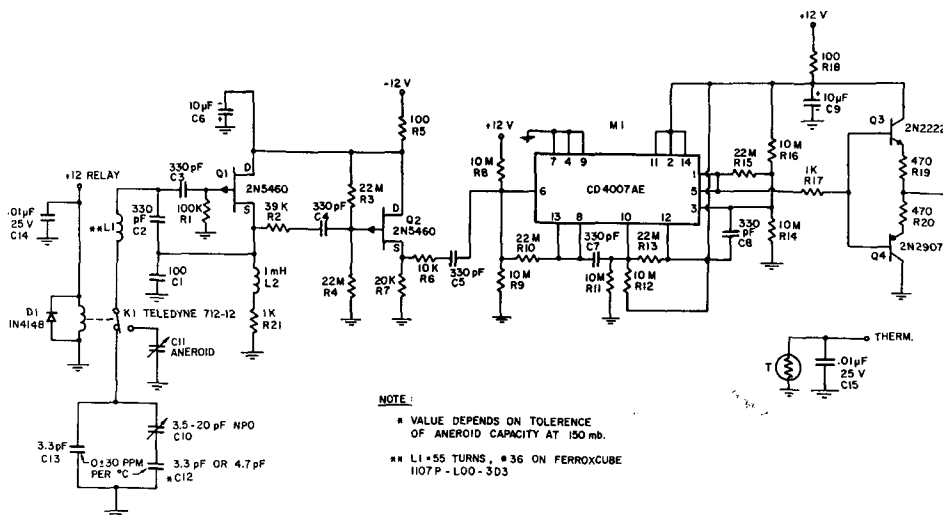


FIG. 4. The pressure sensor electrical schematic diagram.

capacitor and the aneroid capacitor are equal. This nulling occurs at one pressure only, because of the dependence of the aneroid capacitor on the pressure. As shown in the Appendix, 10 mb off the null pressure, an inductance change which will cause a change of 1000 ppm $^{\circ}\text{C}^{-1}$ in the reference frequency, will result in an error of 0.01 mb $^{\circ}\text{C}^{-1}$ in the pressure reading.

b. Compensation

At the null pressure, where the oscillator effect is removed, the only temperature-affected error is caused by the reference capacitor not tracking the aneroid capacitor with temperature. Compensation is obtained by selecting a reference capacitor whose temperature coefficient is equal to the temperature coefficient of the aneroid capacitor. As shown in the Appendix, a difference of 10 ppm $^{\circ}\text{C}^{-1}$ between the two temperature coefficients will result in an error of 0.0125 mb $^{\circ}\text{C}^{-1}$ in the pressure reading.

A typical tolerance of low-cost zero temperature coefficient capacitors is ± 30 ppm $^{\circ}\text{C}^{-1}$. Since this range includes the expected aneroid capacitor temperature coefficient, such capacitors were used in the network of three capacitors which comprise the reference capacitance.

The calibration data from 410 pressure sensors already built gives an average pressure reading temperature dependence of $+0.0615$ mb $^{\circ}\text{C}^{-1}$, with standard deviation of 0.042 mb $^{\circ}\text{C}^{-1}$ from this average. This indicates that, on the average, the temperature coefficient of the reference capacitor used was 50 ppm $^{\circ}\text{C}^{-1}$ more positive than the temperature coefficient of the aneroid capacitor.

c. Temperature measurement

Since the TWERLE package already includes an ambient temperature sensor, no major additions are

required to measure the temperature of the pressure sensor. The pressure sensor thermistor is switched into the temperature measuring circuit, alternating with the ambient temperature sensing thermistor. The specified accuracy of the temperature measuring circuit, when used with a standard thermistor, is $\pm 1^{\circ}\text{C}$. The deviation of the production thermistors from the standard thermistor does not add additional error since the calibration of each pressure sensor is done with its individual thermistor.

d. Temperature packaging

In addition to temperature compensation and measurement, the thermal package of the sensor was designed to minimize temperature changes. It should be noted that the ambient temperature, day and night, may vary from -80°C to -50°C depending on the latitude and the season (Van Loon, 1972). However, during daytime, solar and earth radiation may increase the temperature inside the package to above freezing, depending on the color and the shape of the package. To get a flat dependence on sun angle, a spherical package was selected. In addition, minimum coupling to solar and earth radiation will minimize the night-to-day transition as well as the dependence on sun angle. This minimum coupling was obtained by selecting aluminum foil painted white (normal absorptivity/normal emissivity=0.32) to cover the lower hemisphere, and an aluminum foil covered with mylar ($\alpha_n/e_n=0.5$) to cover the upper hemisphere. The 8-inch sphere is made of styrofoam $\frac{3}{4}$ inch thick.

Typical temperatures of the pressure sensor inside such a spherical package, as taken during four different balloon flights, are given in Fig. 5. These flights were launched from Ascension Island, and the data plotted are from the arrival at ceiling altitude until

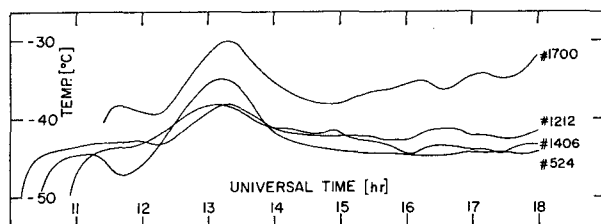


FIG. 5. Temperature of the pressure sensor during the first hours at ceiling from 4 balloon flights. (Ascension Island, 18, 19, 21 and 25 September 1974).

the balloon moved out of the range of the ground station. The typical balloon altitude during these flights was 14.2 km and the typical ambient temperature was -67°C .

4. Adaption and calibration

The evacuated capsule is subjected to mechanical stresses by the external atmospheric pressure. A mechanical creep results which is associated with the accommodation of the crystalline structure to the stress. The effect of the mechanical creep on the pressure reading is to produce a long-term drift (Fink, 1968; Brombacher, 1970).

The first part of the adaption takes place during manufacture at the plant between construction and calibration. The purpose of the first adaption process is to reduce the drift rate to a level which will not distort the calibration data taken at prescribed pressures and temperatures during the 24 h calibration period. This calibration, which is performed by the manufacturer, is actually only a relative calibration. The second part of the adaption, which can also be called aging, takes place between this relative calibration and the pre-launch absolute calibration.

The first part of the adaption is carried out in two phases and is performed with the capsule at its nominal pressure, namely 150 mb. Phase 1 is comprised of exaggerated temperature cycling between -55°C and $+55^{\circ}\text{C}$, to accelerate strain relief. Phase 2 comprises typical temperature cycles, namely -55°C at night and -25°C during the day. Both Phase 1 and Phase 2 are four cycles long. However, if during the 4 cycles of Phase 2 the total change of the 150 mb reading at the -25°C temperature is not less than 0.2 mb, the capsule is returned for an additional adaptation at the Phase 2 level. The length of the adaption phases is a compromise between calibration accuracy and production cost. The calibration is carried out immediately following the last adaption cycle. Frequency differences are measured at five pressures between 170 and 130 mb, at the lowest expected daytime flight temperature of -40°C . These 5 pressure points are repeated at -30°C and at -20°C , the latter being the highest expected daytime sensor temperature. Only after the calibration is performed

at the flight temperature range are two more plots made at $+20^{\circ}\text{C}$ and $+30^{\circ}\text{C}$. These will enable a correction to be made after the pre-launch calibration which will be performed at room temperature. It should be noted that the sensor is soaked at least 4 h at each temperature before the measurements are taken. Furthermore, the exact temperature at which the pressure reading is taken is recorded by measuring the resistance of the pressure sensor thermistor.

The calibration is performed using a precision pressure gauge—Texas Instruments Model 145. The qualities of the gauge which are important for the calibration phase are: i) high sensitivity, ii) servo output to control the tank pressure, and iii) short-term stability to maintain a constant reference pressure during the 24 h calibration phase. There are no special requirements for absolute accuracy during the calibration phase. The requirement for absolute accuracy comes at the pre-launch calibration, which will be discussed later.

At the end of the calibration phase the Lexan bubble that contains the aneroid capsule is pumped down to 100 mb and the relief valve is closed. An additional cork is used to further seal the relief valve if the calibrated sensor is to be stored for a long time before use. Typical bubble leakage is 1 mb day^{-1} and, if not flown within 3 months, the bubble must be pumped down again to 100 mb. Thus, the capsule is kept at the flight pressure of $150\text{ mb} \pm 50\text{ mb}$ from adaption through calibration, storage, shipment, and during most of the balloon ascent.

The pre-launch calibration is performed at the launch site at a pressure of exactly 150 mb, and at the existing ambient temperature. An absolute pressure accuracy is required at this time. The absolute accuracy is achieved by calibrating the TI-145 gauge with a Schwien pressure standard Model 4543-000. This Schwien piston gauge is an air lubricated dead-weight gauge, which is custom built for 150 mb.

The single correction factor obtained during the pre-launch calibration includes the frequency difference reading obtained for 150 mb and the thermistor resistance at which it was taken. The correction factor accounts for any mechanical changes during shipment, the aging during the storage period, and the deviation from absolute of the reference gauge used during the calibration phase. The main reservation with regard to the pre-launch calibration is its relevance if performed at room temperature. Simulation tests with four sensors have shown that the room temperature correction factor is identical to the flight temperature correction factor if the capsule was not exposed to surface pressure for any significant length of time, between the calibration phase and the pre-launch calibration. However, after the capsule was exposed to surface pressure for 41 days, in two out of four sensors, errors of 0.8 and 0.4 mb were introduced. The tests have shown that these errors would not

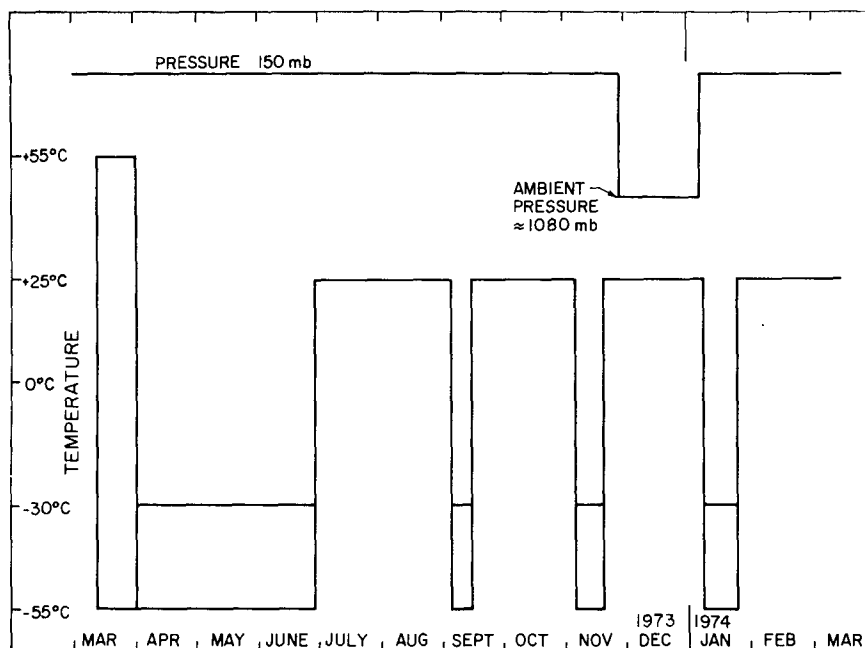


FIG. 6. Temperature and pressure schedule during a 10-month simulation test.

have been introduced had the pre-launch calibration been made at flight temperature after at least two night-day cycles.

5. Simulation tests

Simulation tests were conducted to obtain an estimate of the long-term drift and also to evaluate the pre-launch calibration procedure.

The most extensive life test was performed on 6 prototype pressure sensors, and has lasted 10 months. The testing schedule of the simulation test is summarized in Fig. 6. The adaption (Phases 1 and 2) and the calibration were performed during March 1973. For the next three months the sensors were exposed to simulated flight conditions, namely, temperatures of -55°C night, -30°C day, and a constant pressure of 150 mb. The pressure reading at the -30°C daytime temperature was recorded several times every day. The next two months (July, August, 1973) simulated storage at room temperature with an evacuated bubble (150 mb). Then the normal flight conditions were resumed for two weeks with the pressure reading taken during the daytime part (-30°C) of the cycle. On 20 September the sensors were brought up again to $+25^{\circ}\text{C}$ (150 mb maintained). However, this time, the readings of the 150 mb pressure were taken for 5 consecutive days, suspended for about 1 month, and then resumed for 5 more consecutive days. The difference in pressure reading was equivalent to the correction factor. On 5 November the sensors were brought back to flight conditions with the 150 mb readings taken again several times every day during

the daytime part (-30°C) of the cycle. The differences between these pressure readings and the pressure readings taken during the previous flight condition simulation period 6 September to 18 September should be equal to the correction factor obtained at $+25^{\circ}\text{C}$, if the procedure of measuring the correction factor at room temperature is acceptable. The 6 September to 13 November 1973 pattern was repeated again between 7 November 1973 and 18 January 1974. However, this time, during the $+25^{\circ}\text{C}$ phase, the pressure was brought up to surface pressure (approximately 1080 mb) for 41 days. A numerical value for the correction factor in this case was also obtained.

The results of the tests for one sensor, #104, are given in Figs. 7, 8 and 9. The results for the remaining sensors are given in Table 1. Fig. 7 is an overview of the entire 10-month test. All of the readings are for 150 mb pressure as controlled with the help of the TI-145 gauge. The drift of the TI gauge was not measured. Subsequent experience with five such gauges produced drift rates between 0 to 2 mb per year at 150 mb.

The outstanding features of sensor #104 are an initial drift of 0.5 mb per 3 months of flight conditions (April, May and June). This drift of $+0.5$ mb was compensated by -0.5 mb during the $+25^{\circ}\text{C}$ periods. The final readings of flight conditions (January 1974) were only 0.2 mb below the first readings taken in April 1973.

Fig. 8 is an expanded section of Fig. 7 for the period 6 September to 14 November, 1973, confirming the validity of obtaining the correction factor at room temperature if the sensor being stored at room tem-

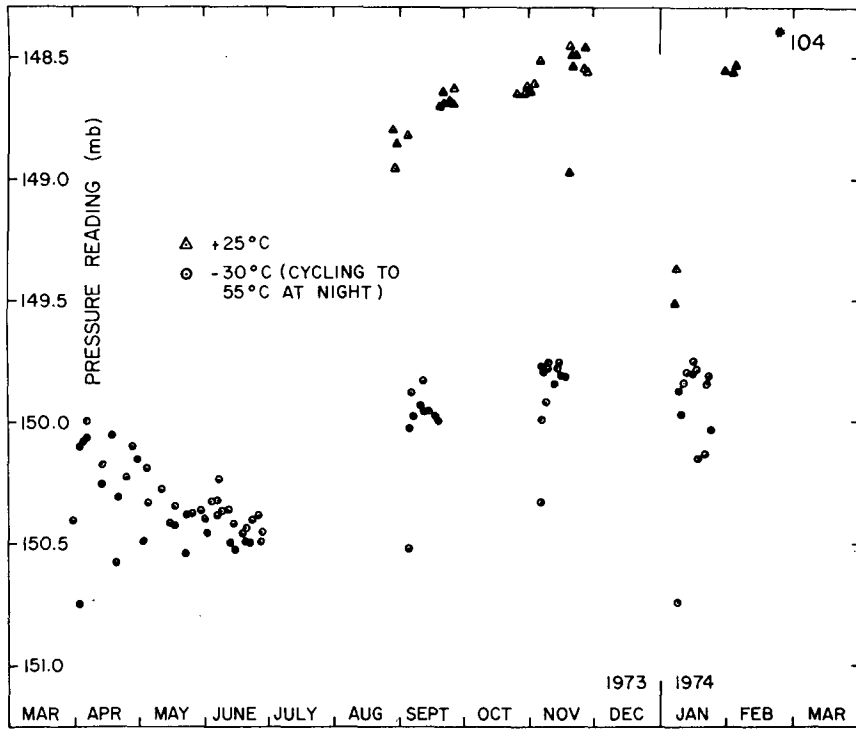


FIG. 7. Pressure readings during the 10-month simulated test (true pressure 150 mb as controlled by TI-145 gauge). Sensor # 104.

perature (+25°C) is maintained at flight pressure (150 mb).

Fig. 9 is an expanded section of the 7 November 1973 to 18 January 1974 period, where the storage

pressure was brought up to surface pressure (1080 mb). Here a correction factor at +25°C was +0.8 mb while the correction factor at -30°C was 0 mb.

The results from the correction factor tests appear

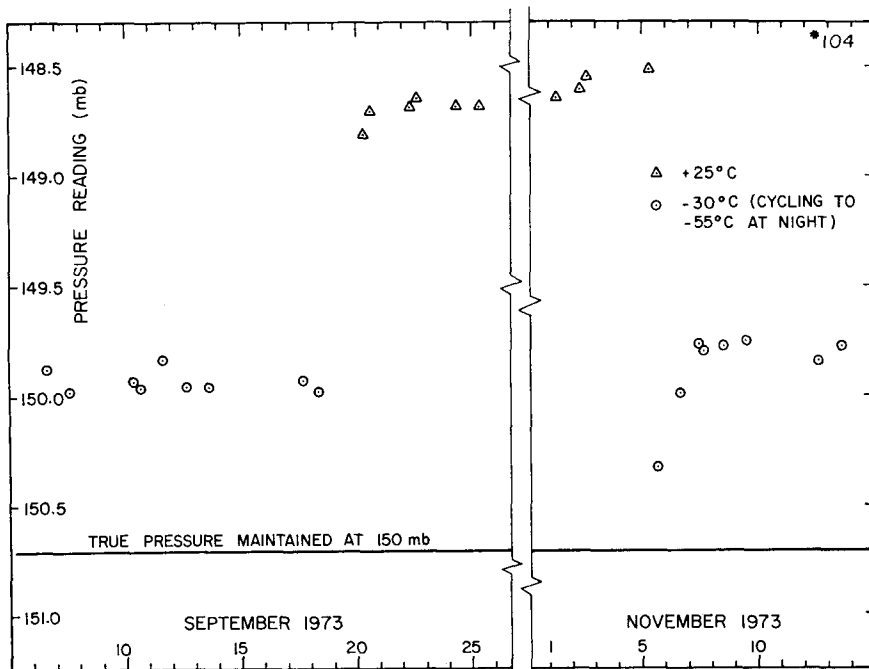


FIG. 8. Expanded section of Fig. 7 (6 September-14 November 1973).

TABLE 1. Summary of simulation tests on prototype pressure sensors.

Sensor no.	102	103	104	105	106	108
Accumulated drift during May-June 1973	+0.4 mb	+0.4	+0.4	+0.3	+0.5	+0.25
Accumulated drift May-Sept. 1973	+0.1 mb	+0.1	-0.2	-0.3	+2.8	0
Accumulated drift May 1973-Jan. 1974	+0.6 mb	+0.5	-0.3	Not available	+3.5	+0.3
Correction factors:						
Sept.-Nov. 1973 +25°C	0 mb	0	-0.1	0	0	+0.2
-30°C	0 mb	0	-0.1	-2	+0.1	+0.3
Nov. 1973-Jan. 1974 +25°C	0 mb	+0.4	+0.8	+2	0	Not available
-30°C	0 mb	0	0	-0.5	0	Not available

also in Table 1. The conclusion with regard to the correction factor is that it can be measured at room temperature only if storage of the sensor was at flight pressure.

A second simulation test was conducted during the production process. Four sensors from the first production group were kept in the pressure/temperature chamber and were subjected to five more adaption and calibration cycles. The total drift for these sensors, observed from the original calibration to the final calibration 108 days later, is summarized in Table 2. The estimated drift of the TI-145 gauge used in the above test is based on the assumption that the gauge was accurate at the beginning of the test when it had just arrived from the factory. Toward the end of the test this gauge was compared to two other gauges which have been returned from recalibration at the factory. The comparison indicated calibration changes of +0.46 mb and +0.77 mb respectively.

The main difference between the simulation tests conducted on the production units and the one conducted on the prototypes is that the production units were exposed to 5x4 cycles of +55°C to -55°C, i.e., farther away from the expected flight conditions.

TABLE 2. Drift of production pressure sensors during 5 repetitions of the adaption and calibration phases (108 days).

Sensor no.	85	86	87	88
Sensor drift	+1.3 mb	+1.2	+3.2	+0.7
Estimated TI-gauge drift	+0.6 mb	+0.6	+0.6	+0.6
Estimated sensor drift	+0.7 mb	+0.6	+2.6	+0.1

It is again emphasized that all of the results on the long-term drift, should be considered as estimates only, owing to the lack of a true absolute calibration of the reference pressure gauge (TI-145).

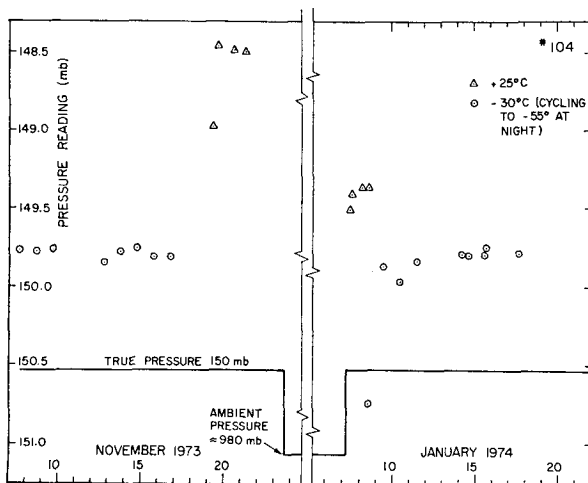


FIG. 9. Expanded section of Fig. 7 (7 November 1973-18 January 1974).

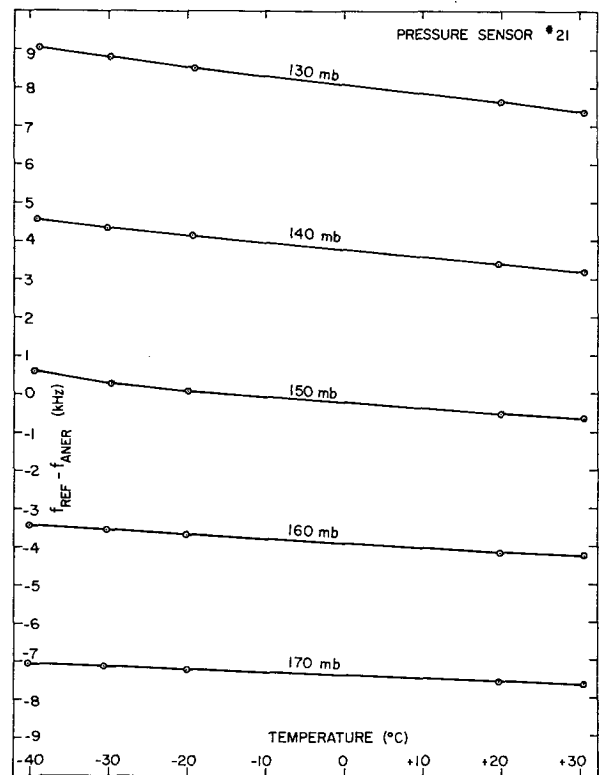


FIG. 10. Calibration data from a typical production pressure sensor (#21).

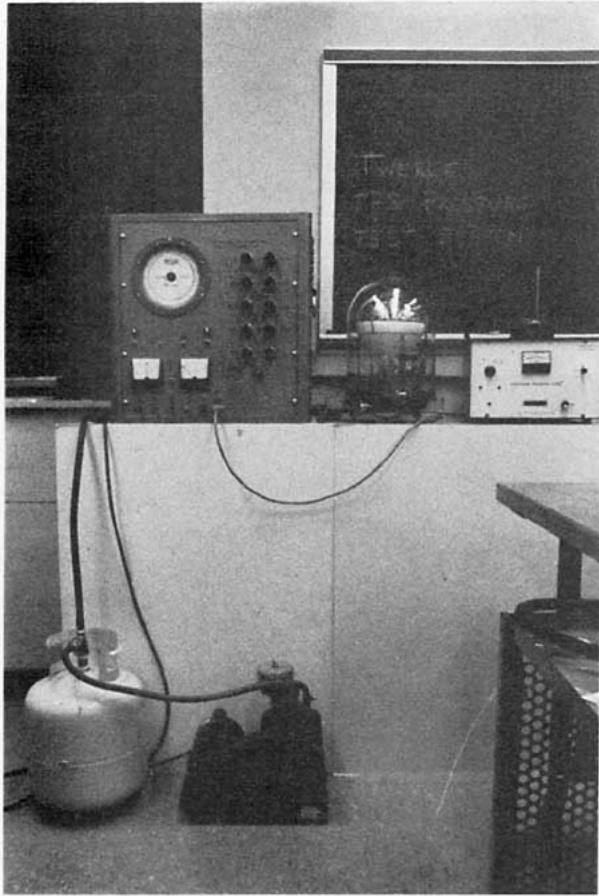


FIG. 11. Launch site pressure sensor test system.

TABLE 3. Temperature dependence averages for 411 sensors.

	Average	Standard deviation
Sensitivity ($f_{ref} - f_{aver}$) @ 150 mb, -30°C	-419.5 Hz mb ⁻¹	42.8 Hz mb ⁻¹
Temperature dependence @ 150 mb, -30°C	0.0615 mb °C ⁻¹	0.0419 mb °C ⁻¹

6. Production and flight tests results

Calibration data from a typical production pressure sensor are given in Fig. 10. The 25 data points that comprise the calibration information for each sensor are stored on magnetic tapes for subsequent conversion of the frequency and the sensor temperature data, transmitted by the balloon, to pressure.

Based on the calibration data from 411 pressure sensors, the averages and standard deviations which have been found are given in Table 3.

The above sensitivity numbers indicate excellent reproducibility of the pressure sensors. The temperature dependence numbers indicate that the compensation is not perfect, but sufficient, since the sensor temperature is known within 1°C.

In 10 test flights launched from Christchurch, New Zealand, in February, March 1974 and from Ascension Island in September 1974, the correction factors found in the pre-launch calibration were within -0.9 mb ±0.55 mb. The launch site pressure test system is shown in Fig. 11. The pressure information from a

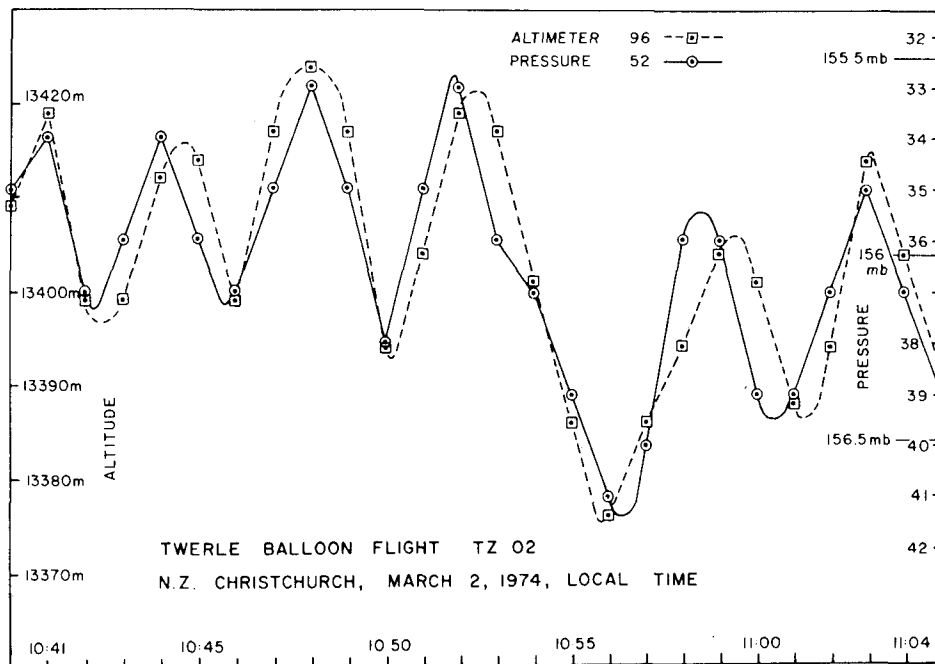


FIG. 12. Pressure and altitude readings from a constant level balloon flight (2 March 1974, Christchurch, N. Z.).

section of 25 min during one of the Christchurch flights (2 March) is given in Fig. 12. The pressure readings are plotted together with the balloon-borne radio altimeter readings to demonstrate the excellent agreement between these two different instruments, and also to indicate how the altitude of a pressure reference level is obtained.

For two of the Christchurch flights (2 March and 5 March) we have a comparison between the reference level, as measured by the TWERLE pressure sensor and altimeter, and the reference level as calculated from radiosonde soundings. The results are given in Table 4.

On both days the radiosonde reference level is 25 m above the one measured by the TWERLE sensors. The difference is too small to resolve the individual errors contributed by each of the TWERLE sensors or by the radiosonde.

7. Conclusions

The pressure sensor to be used in the TWERLE Experiment has been described. Various techniques to improve accuracy using radiosonde type aneroid capsules were discussed. Full advantage was taken of the constant level application by nullifying the oscillator effect at the expected flight pressure, and by storing the sensor at that pressure. The main remaining source of error is the long-term drift of the stressed capsule. During the TWERLE flight, control sensors will undergo simulated flight conditions to obtain an additional estimate of the drift. For future experiments, if cost permits, different materials should be investigated (e.g., quartz) that are less susceptible to drift.

It is hoped that users of the TWERLE data will obtain from this paper an insight into the pressure sensor as well as a true estimate of the level of confidence to be associated with the pressure readings.

Acknowledgments. The authors wish to acknowledge the contribution of the late John A. Kruse to the development of the sensor.

Thanks are due to C. Wolfe of Boulder Scientific Research and Development Laboratory, Inc., for his efforts in the manufacturing of the sensors; to E. W. Lichfield, J. Tefft, and V. E. Lally of NCAR for many balloon tests; and to C. Morel and D. Shea, also of NCAR, for calibration data processing and analysis.

The TWERLE Experiment, for which this sensor was developed, is supported by the National Aeronautics and Space Administration and the National Science Foundation and is administered by the University Corporation for Atmospheric Research.

TABLE 4. Reference levels as measured by TWERLE sensors compared to levels obtained by radiosonde sounding.

Pres- sure (mb)	Flight number, date and time			
	TZ02		TZ03	
	2 March 1974		5 March 1974	
	1100		1050	
	Altitude (m)		Altitude (m)	
	TWERLE	Radio- sonde	TWERLE	Radio- sonde
153	—	—	13825	13848
154	—	—	13780	13807
155	13445	—	13735	—
156	13404	—	—	—
157	13362	13387	—	—
158	13321	13346	—	—

APPENDIX

The Effect of the Oscillator Circuitry on the Pressure Reading

The frequency determining network of the oscillator can be simplified to an L-C circuit with C being either the reference capacitor C_r , or the aneroid capacitor C_a , and L being the effective inductance of the oscillator. The reference frequency, f_r , and the aneroid frequency, f_a , are given as

$$f_r = \frac{1}{2\pi\sqrt{LC_r}} \tag{A1}$$

$$f_a = \frac{1}{2\pi\sqrt{LC_a}} \tag{A2}$$

The two capacitors are found from the respective frequencies

$$\sqrt{C_r} = \frac{1}{2\pi f_r \sqrt{L}} \tag{A3}$$

$$\sqrt{C_a} = \frac{1}{2\pi f_a \sqrt{L}} \tag{A4}$$

The pressure-dependent frequency is the difference frequency f_d defined as

$$f_d = f_r - f_a \tag{A5}$$

1) Assume first that only the coil inductance changes by an amount ΔL . Both frequencies now have a new value, namely,

$$f_r^* = \frac{1}{2\pi[(L-\Delta L)C_r]^{\frac{1}{2}}} \tag{A6}$$

$$f_a^* = \frac{1}{2\pi[(L-\Delta L)C_a]^{\frac{1}{2}}} \tag{A7}$$

and a new pressure-dependent-frequency reading will

result:

$$f_d^* = f_r^* - f_a^*. \quad (\text{A8})$$

Substitution of (A6) and (A7) into (A8) yields

$$f_d^* = \frac{\sqrt{C_a} - \sqrt{C_r}}{2\pi[(L - \Delta L)C_a C_r]^{\frac{1}{2}}}. \quad (\text{A9})$$

Substitution of (A3) and (A4) in (A9) and using (A5) yields

$$f_d^* = f_a \frac{f_r^*}{f_r}. \quad (\text{A10})$$

(A10) can be rewritten as

$$f_d^* - f_d = f_a \frac{f_r^* - f_r}{f_r}, \quad (\text{A11})$$

or as

$$\Delta f_d = f_a \frac{\Delta f_r}{f_r}, \quad (\text{A12})$$

where

$$\Delta f_d = f_d^* - f_d \quad (\text{A13})$$

is the change in the pressure-dependent-frequency, i.e., the error, and

$$\Delta f_r = f_r^* - f_r \quad (\text{A14})$$

is the change in the reference frequency caused by a change in the effective inductance of the oscillator. Eq. (A12) indicates that, at the pressure where the reference frequency equals the aneroid frequency

($f_d=0$), changes in the effective inductance of the oscillator will not have any effect on the pressure reading. The reference capacitor is hence set for $f_d=0$ at the expected flight pressure of 150 mb. Ten millibars off that null pressure, and with a typical sensitivity of the sensor of -400 Hz mb^{-1} a change in the effective inductance that will cause a change of 1000 ppm in the reference frequency will result in an error of only 0.01 mb.

2) We will now assume that only the reference capacitance changes, by an amount ΔC_r . From (A1) we get

$$\Delta f_r = -\frac{1}{2} \frac{\Delta C_r}{C_r} f_r. \quad (\text{A15})$$

Since C_a and f_a did not change, we get from (A5) that

$$\Delta f_d |_{\Delta f_a=0} = \Delta f_r. \quad (\text{A16})$$

Using for $\Delta C_r/C_r$ the value $+10 \text{ ppm } ^\circ\text{C}^{-1}$ and the typical value of $f_r = 1 \text{ MHz}$, we get from (15) and (16) that $\Delta f_d = -5 \text{ Hz } ^\circ\text{C}^{-1}$. With a typical sensitivity of -400 Hz mb^{-1} , a change in f_d of $-5 \text{ Hz } ^\circ\text{C}^{-1}$ will be equivalent to a pressure reading change of $+0.0125 \text{ mb } ^\circ\text{C}^{-1}$.

REFERENCES

- Brombacher, W. G., 1970: *Survey of Micromanometers*. NBS Monograph 114, 62 pp.
 Fink, C., 1968: *Über aneroid-dosen für radiosonden*. Munich, German Weather Service, Instruments Bureau.
 Van Loon, H., 1972: Temperature in the Southern Hemisphere. *Meteor. Monogr.*, 13, No. 35, 25-58.